

Impact of the Energy Landscape on the Ionic Transport of Disordered Rocksalt Cathodes

Shashwat Anand, Tina Chen, and Gerbrand Ceder*

Materials Sciences Division, Lawrence Berkeley National Laboratory, Berkeley, CA 94720, USA

(Dated: January 27, 2023)

Traditional approaches to identify ion-transport pathways often presume equal probability of occupying all hopping sites and focus entirely on finding the lowest migration barrier channels between them. Although this strategy has been applied successfully to solid-state Li battery materials, which historically have mostly been ordered frameworks, in the emerging class of disordered electrode materials some Li-sites can be significantly more stable than others due to a varied distribution of transition metal (TM) environments. Using kinetic Monte Carlo simulations, we show that in such cation-disordered compounds only a fraction of the Li-sites connected by the so-called low-barrier “0-TM” channels actually participate in Li-diffusion. The Li-diffusion behavior through these sites, which are determined primarily by the voltage applied during Li-extraction, can be captured using an effective migration barrier larger than that of the 0-TM barrier itself. The suppressed percolation due to cation disorder can decrease the ionic diffusion coefficient at room temperature by over 2 orders of magnitude.

Until recently, candidate materials studied for Li battery electrode applications have predominantly been ordered compounds.[1] A separation of sublattices on which Li and transition metal (TM) reside was considered essential for unhindered ionic transport in electrode materials. Commercialized layered cathodes — an example of such ordered materials — therefore use only a few TMs (e.g. Ni, Co and Mn) which have the proper electronic structure to accommodate and retain the layered ordering for hundreds of cycles.[2] This constraint on the choice of metals has set the Li-ion battery industry on a path to consume a sizable fraction of the world’s annual Co/Ni production if energy storage goals of > 1 TWh/year are to be met.[3, 4]

The recent development of Li-excess cation-disordered rocksalt (DRX) cathodes[5–9], in which Li and other metals are disordered over the octahedrally coordinated sites in a rocksalt structure, lifts the restriction on a specific Li-TM ordering to enable the exploration of cathode materials in a much wider chemical space. In general, DRX cathodes are known to show high capacity[10, 11] and good stability.[12–14] Some DRX compounds[15, 16] as well as similar disordered materials with partial spinel-like features[17] have also shown exceptional rate capability. DRX compounds are also being studied as potential anode materials.[18] But this evolution of electrode materials towards disordered materials necessitates the development of new models[19] to understand the more complex ion transport through a disordered environment. While the basic transport theory in cation disordered rocksalts has been developed through percolation models, we show in this paper that a more rigorous understanding requires consideration of the varying site energy landscape of the Li-sites, and that in general this effect leads to a substantial reduction in Li-ion mobility.

In close-packed oxides, the Li-ion resides in the oxygen octahedra (O_h) and migrates through intermediate face-sharing tetrahedral sites (T_d). In DRX cathodes, Li migration occurs through low-barrier Li-rich tetrahedral environments (0-TM channels, where the tetrahedral site does not face-share with any transition metal or TM) as this provides a low electrostatic repulsion pathway for migration (Figure 1 a). Therefore, Li-excess compositions ($x > 0.1$ in $Li_{1+x}TM_{1-x}O_2$) in which all the 0-TM channels are connected as a percolating network[20] are expected to boost rate capability and maximize reversible capacity. Compared to 1-TM channels for diffusion, through which Li-migration in layered cathodes occurs, the migration barriers for 0-TM channels in DRX compounds are generally much smaller and should lead to ionic diffusion at least two orders of magnitude faster.[5] Despite this, measured values of Li-diffusivity in DRX compounds (10^{-15} $cm^2 s^{-1}$)[16, 21, 22] are often a few orders of magnitude smaller than that of layered compounds (10^{-8} $cm^2 s^{-1}$ - 10^{-13} $cm^2 s^{-1}$) with occasional measurements[23] reported in a comparable range. Barring a few exceptions, Li-excess DRX cathodes mostly show limited rate capability, which may be connected to poor Li-ion diffusion. Therefore, the current understanding of Li transport based entirely on 0-TM percolation is used largely only for qualitative comparisons of Li diffusion and rate capability between compounds. [15, 21]

The traditional percolation theory focuses on understanding Li-transport pathways by ensuring connectivity of the low energy intermediate T_d sites. However, the cation disorder in DRX compounds also lead to a varied TM environment, which influences the energies of Li O_h sites. Li transport therefore will not depend only on the (T_d) site environments (0-TM, 1-TM and 2-TM) but also on local variations in site energy. The sketch in Figure 1 b contrasts the migration barrier (E_a) associated with a Li hop in the DRX compounds with that in ordered compounds in the dilute carrier limit. While in ordered compounds the surrounding TM environments of the Li

* gceder@berkeley.edu

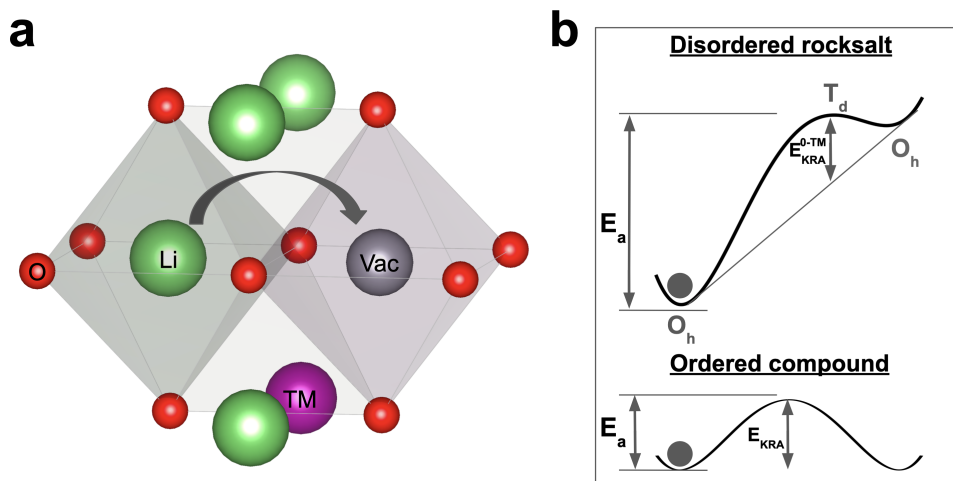


FIG. 1. (a) 3D view of 0-TM and 1-TM tetrahedral diffusion channels between adjacent edge sharing Li-sites in DRX compounds. The lower barrier 0-TM channel (black arrow) forms the basis of the percolating Li pathway. (b) Activation barrier E_a associated with hopping out of an occupied octahedral (O_h) site in a DRX system versus a typical ordered compound. Even with the same kinetically resolved activation barrier (E_{KRA}), E_a in DRX systems can be much larger due to a difference in the O_h site energies.

sites are mostly the same, the site energies of the O_h Li sites in the DRX compounds vary causing the migration barrier to change depending on the initial and final positions of the Li-ion. As a result of such a varied energy landscape, the migration barrier of 0-TM channels in DRX compounds can vary significantly and a percolation analysis based on 0-TM connectivity alone — although applicable to ordered counterparts — may not be sufficient. For larger variations in site energy, some sites cannot be occupied, limiting the Li-sites in the 0-TM percolating network that can participate in ionic transport.

The effect of varying site energies on Li-transport can be isolated by defining a kinetically resolved activation (KRA) barrier E_{KRA} , [24] which represents the contribution from the T_d site environment (E_{KRA}^{0-TM} for 0-TM channels) to the overall magnitude of the migration barrier E_a . E_{KRA}^{0-TM} is obtained by subtracting the average of the energies for the end points of the hop from the energy at the activated state T_d as shown in Figure 1 b. Here, we study Li-transport in a model DRX system keeping E_{KRA}^{0-TM} constant and varying the extent of variance in the Li site energies.

In this paper we perform kinetic Monte Carlo (KMC) simulations to calculate Li-diffusion within a simplified model which includes varying site energies, mimicking the Li-TM site disorder as well as nearest neighbor Li-Li interactions. We show that in disordered cathodes where the standard deviation in Li site energy distribution (w_{SE}) is much larger than the thermal energy ($k_B T$), traditional percolation theory is not sufficient for understanding Li transport. Due to the larger migration barriers associated with the escape from lower-energy sites, only a fraction of the Li-sites within the 0-TM percolating network actually participate in ionic transport at a given voltage (which sets the Li content and average en-

ergy of Li-ions). In real DRX materials we find that the magnitude of w_{SE} can be comparable to E_{KRA}^{0-TM} itself, and the impact of cation disorder in limiting Li percolation is sufficient to suppress the room temperature diffusion coefficient by over 2 orders of magnitude.

To investigate the effect of a disordered energy landscape on cation diffusion, we construct a model system with a single FCC lattice on which Li and vacancies (Vac) are the only two species allowed. The transport properties in this model system are calculated with varying Li occupancies (x_{Li}) in the range [0,1]. To mimic the interactions between Li and TM atoms in a system, the Li site energy is varied according to a Gaussian distribution with standard deviation w_{SE} . The Li site energy landscape was kept static during Li diffusion to simulate a fixed TM environment (topotactic process). The interaction between Li sites is limited in the model to nearest neighbors and is accounted for using the effective cluster interaction J_{Li-Vac}^{NN} (see supplementary material) [25]. Kinetic Monte Carlo simulations [26, 27] were performed using a rejection-free algorithm [28, 29] to determine the tracer diffusion coefficient (D) and the correlation factor f .

To isolate the effect of the varying O_h site energy distribution on Li-diffusion, the tracer diffusion coefficient was calculated for $J_{Li-Vac}^{NN} = 0$ and constant E_{KRA}^{0-TM} with w_{SE} varied in the range [0 eV, 1 eV]. The calculated D at different Li occupancies is shown in Figure 2a. Data corresponding to larger w_{SE} values are shaded with darker symbols and data for the extreme w_{SE} values are connected by solid lines. In general, we find that the variance in O_h site energy distribution suppresses the diffusion coefficient at all Li compositions. In the non-dilute regions, the diffusion coefficient decreases by over 4 orders of magnitude for $w_{SE} = 1$ eV in comparison to the or-

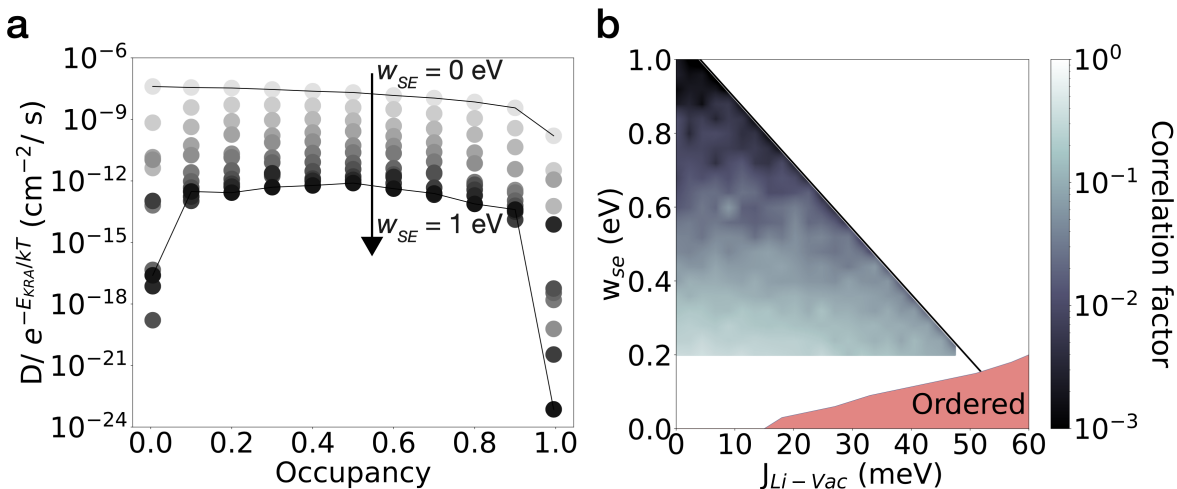


FIG. 2. (a) Impact of varying O_h site-energy distribution (standard deviation w_{SE}) on the calculated Li diffusion coefficient at different occupancy of the O_h sites. The magnitude of w_{SE} , represented by the shade of the data points, is varied over 11 values in the range [0 eV, 1 eV]. (b) Contour plot of calculated correlation factor (f) at $x_{Li} = 0.3$ in the 2-dimensional parameter space (w_{SE} , J_{Li-Vac}^{NN}) of the model system. The parameters which best fit the experimentally measured voltage profile of $\text{Li}_{1.17-x}\text{Mn}_{0.343}\text{V}_{0.486}\text{O}_{1.8}\text{F}_{0.2}$ are given by the solid black line. The region in which the model system becomes ordered at room temperature ($T = 300$ K) is shaded in salmon.

dered compound ($w_{SE} = 0$ eV). The impact of cation disorder is much more pronounced in the dilute limit where D is reduced by over 10 orders of magnitude at $w_{SE} \sim 1$ eV.

To gain insights into the origin of the large drop in D with w_{SE} , we inspect the corresponding calculated correlation factor (f), which is a measure of the degree to which successive hops of the diffusing species are correlated ($f = 1$ for non-interacting particles performing random walk).[30, 31] In variants of the rock-salt compounds with layered cation ordering such as Li_xCoO_2 , f is typically $> 10^{-1}$, except at values of x approaching 1.[27] Calculated $f \sim 1$ for $w_{SE} = 0$ eV and $J_{Li-Vac}^{NN} = 0$ meV in the model signify an unhindered random walk because successive Li-hops have no correlation between them. In Figure 2 b, the correlation factor as a function of w_{SE} and J_{Li-Vac}^{NN} at $x_{Li} = 0.3$ and $T = 300$ K using a color scale. The region corresponding to ordered Li-Vac configurations in the model is shaded salmon (see supplementary information) and is not relevant here. The solid line exemplifies the possible relative magnitudes of w_{SE} and J_{Li-Vac}^{NN} in real DRX systems as estimated by comparing the calculated voltage profile for the model with the experimentally measured voltage profile for $\text{Li}_{1.17-x}\text{Mn}_{0.343}\text{V}_{0.486}\text{O}_{1.8}\text{F}_{0.2}$ (see discussion below). We find that by increasing w_{SE} alone, as in Figure 2 a, f is suppressed by three orders of magnitude, suggesting a strong correlation between successive hops. Although f is suppressed with increasing J_{Li-Vac}^{NN} as well, its effect on f appears much weaker than that of w_{SE} . For $w_{SE} \sim 0.2$ eV, f is of the same order of magnitude as Li_xCoO_2 at similar Li-concentration ($x = 0.3$), suggesting that this extent of site energy variation does not have a very adverse impact on Li-diffusion.

To understand the impact of cation disorder on Li site percolation, we compare in Figure 3 the site energy distribution of all Li sites (blue histogram, left y-axis) against the energy distribution of those sites that actually participate in diffusion (yellow, orange, green histograms, right y-axis) at room temperature for different values of x_{Li} . The solid red curve represents the Gaussian distribution curve with the same standard deviation as the w_{SE} ($= 0.8$ eV) used in the model. We find that most of the transport occurs predominantly through Li sites with site energies falling within a few $k_B T$ of the highest energy occupied Li site. All vacant sites above this range and occupied sites below it are effectively immobile due to the prohibitively large migration barriers connecting nearest-neighbors with relatively larger site energy differences. For the model system with $w_{SE} = 0.8$ eV, the sites participating in transport for $x_{Li} = 0.2, 0.5$ and 0.8 are almost entirely different from each other. These results show that during delithiation, the sites available for transport will depend on the voltage applied and can be severely limited when $w_{SE} \gg k_B T$. As a result, the fraction of Li sites available for percolation can effectively be much smaller than that expected from the 0-TM channel connectivity[20] for a given x in $\text{Li}_x\text{TM}_{1-x}\text{O}_2$.

To capture the effect of the varied O_h energy landscape on the overall Li diffusion, an Arrhenius plot of D for multiple w_{SE} is shown in Figure 4 (for $x_{Li} = 0.3$). Note that values of D are normalized by $\exp\left(\frac{-E_{KRA}}{k_B T}\right)$ to isolate the effect of the site energy distribution on the activation energy. Consistent with the calculations for room temperature in Figure 2, D is suppressed at all temperatures with increasing w_{SE} . In the high temperature limit, D displays an Arrhenius behavior varying as

$D \propto \exp\left(\frac{-E_a}{k_B T}\right)$ and suggests that the transport through 0-TM channels can still be modeled with a single *effective* activation barrier (E_a^{eff}), which approximately behaves as $E_a^{\text{eff}} \sim E_{\text{KRA}} + 0.45w_{\text{SE}}$. At lower temperatures, the diffusion coefficient gradually deviates from this behavior, signifying a smaller effective activation barrier caused by the participation of sites lying in a narrower energy window. Importantly, Figure 4 shows that, unlike in ordered compounds, $E_a \neq E_{\text{KRA}}$ in disordered materials even when nearest neighbor Li-Vac interactions are absent ($J_{\text{Li-Vac}}^{\text{NN}} = 0$ eV). Furthermore, results in Figure 4 suggest that $E_a^{\text{eff}} > E_{\text{KRA}}^{0\text{-TM}}$ and E_a^{eff} lies quite close in range to $E_{\text{KRA}}^{1\text{-TM}}$ (typically $E_{\text{KRA}}^{1\text{-TM}} - E_{\text{KRA}}^{0\text{-TM}} \sim 0.2$ eV [14]), and 1-TM channels could therefore also participate in ionic-transport.

The typical value for $J_{\text{Li-Vac}}^{\text{NN}}$ used in our model can be expected to be similar to that of the layered variants

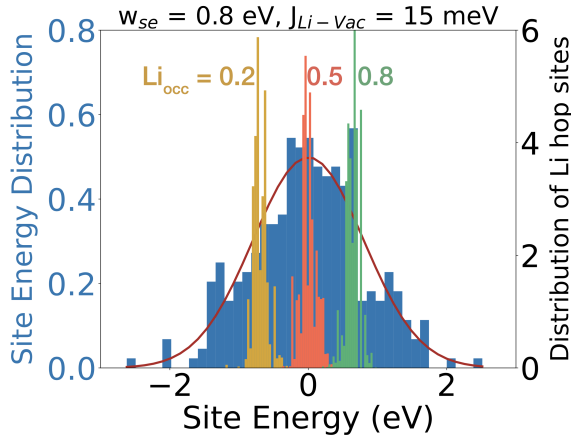


FIG. 3. Li site energy distribution (blue histogram) with standard deviation $w_{\text{SE}} = 0.8$ eV. Distribution of Li sites involved in Li-diffusion at $x_{\text{Li}} = 0.2, 0.5, 0.8$.

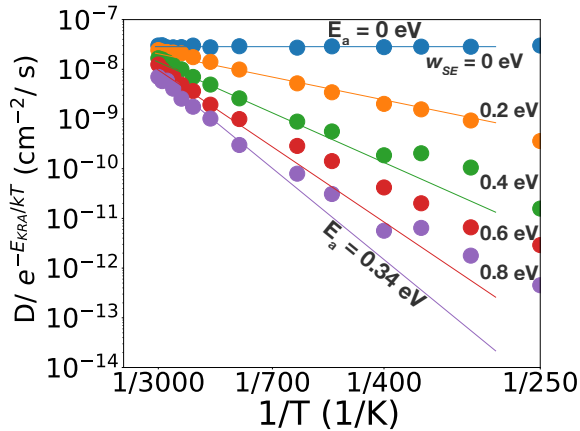


FIG. 4. Arrhenius plot of calculated tracer diffusion coefficient for model DRX systems at $x_{\text{Li}} = 0.3$ with varying w_{SE} in the range $[0, 0.8]$. Corresponding high temperature data is fitted by an increasing effective activation barriers of magnitude $\sim E_{\text{KRA}} + 0.45 w_{\text{SE}}$.

of the rock-salt type crystal structure, where $J_{\text{Li-Vac}}^{\text{NN}} \sim 15\text{-}35$ meV [32, 33]. Physically reasonable values of w_{SE} in DRX compounds can then be gauged by comparing the model's calculated voltage profile to experimentally measured voltage profiles. Figure 5 shows an example for such a comparison of the $\text{Li}_{1.17-x}\text{Mn}_{0.343}\text{V}_{0.486}\text{O}_{1.8}\text{F}_{0.2}$ experimental profile with the calculated voltage profile at $w_{\text{SE}} = 0.6$ eV and $J_{\text{Li-Vac}}^{\text{NN}} = 25$ meV. Because both $J_{\text{Li-Vac}}^{\text{NN}}$ and w_{SE} contribute to the slope of the calculated voltage profile ($\frac{dV}{dx_{\text{Li}}}$), [34] a series of values for them exist that will lead to the same voltage slope, which for $\text{Li}_{1.17-x}\text{Mn}_{0.343}\text{V}_{0.486}\text{O}_{1.8}\text{F}_{0.2}$ is shown in Figure 2b by the solid line. Since the slope of the $\text{Li}_{1.17-x}\text{Mn}_{0.343}\text{V}_{0.486}\text{O}_{1.8}\text{F}_{0.2}$ voltage profile is one of the largest among experimentally measured DRX compounds, the corresponding values of w_{SE} and $J_{\text{Li-Vac}}^{\text{NN}}$ can be expected to be almost an upper limit for DRX compounds. We note that the Li-site energy landscape could also depend on variations in charge of the cation environment with Li-extraction (e.g. $\text{Mn}^{3+} \rightarrow \text{Mn}^{4+}$) as well as the redox chemistry of the transition metal involved. As a result, comparisons like the one shown in Figure 5 can only provide approximate estimates of w_{SE} , and voltage profiles calculated with system-specific cluster expansions could provide more insight into the Li-site energy landscape of DRX compounds. [30, 35]

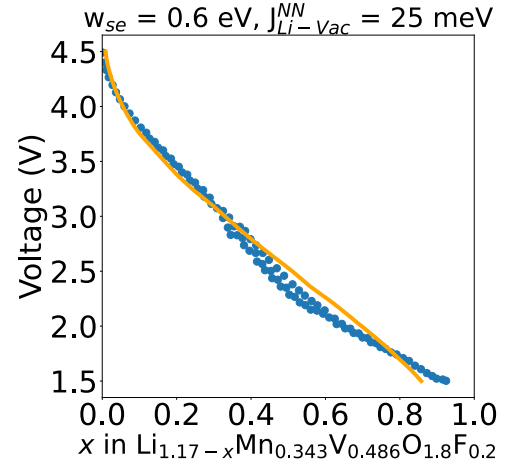


FIG. 5. Calculated voltage profile for model DRX system with $w_{\text{SE}} = 0.6$ eV and $J_{\text{Li-Vac}}^{\text{NN}} = 25$ meV fit to the experimentally measured voltage profile of $\text{Li}_{1.17-x}\text{Mn}_{0.343}\text{V}_{0.486}\text{O}_{1.8}\text{F}_{0.2}$.

Despite its approximate nature, our analysis can be used to develop general guidelines for correlating the rate capability of disordered cathode materials to their voltage profile. Since increasing either $J_{\text{Li-Vac}}^{\text{NN}}$ or w_{SE} suppresses Li-diffusion and increases the slope of the voltage profile, one can expect rate capability to be better for materials with a flatter voltage profile. An example of this behavior can be found in partially disordered Li-excess spinel materials $\text{Li}_{1+x+y}\text{Mn}_{2-y}\text{O}_4$ for which the rate capability and voltage profiles were studied with varying x and fixed Mn content. [36] The rate capability was found

to be better for compounds with relatively flatter voltage profiles, suggesting that the improved performance — besides a larger fraction of kinetically accessible Li through 0-TM percolation — could be caused by the smaller degree of disordering in them.

In addition to cation disorder, disorder on the anionic sub-lattice (F^- , O^- and O^{2-}) due to the occurrence of O redox mechanism[37–41] or fluorination[14, 42] may also effect ionic transport by modifying the the Li-site energy landscape. For instance, fluorination has been shown to increase the asymmetry of migration barriers in o-LiMnO₂ by over 100 meV due to changes in local Li site energy, although it had minimal effect on the E_{KRA} . [43] Besides anion disorder, our analysis for DRX compounds could in principle also be extended to describe ionic transport in (i) compounds containing mobile TM elements such as Cr which undergo reversible octahedral-to-tetrahedral (oct-tet) migration during electrochemical cycling[16] and (ii) partially disordered spinel compounds[44], where the T_d and O_h site energy distributions overlap to cause a rearrangement of Li-occupancy.

In conclusion, we specifically identify the effect of the varied TM environment seen by Li-sites in DRX compounds on ionic transport. This effect of Li-TM interactions is isolated by calculating diffusion coefficients for increasing variances in Li-site energy distributions and contrasted with that of Li-Vac interaction. We find that, for a DRX compound with a given voltage profile, the im-

port of Li-TM interactions on suppressing the diffusion coefficient can be much stronger than that of the Li-Vac interactions. Suppressed Li-diffusion occurs despite the connectivity of Li-sites through a network of 0-TM channels and results in part from effectively “immobile” Li-ions, which reside in sites with significantly lower energy than the Li-ions that participate in transport. Therefore, in comparison to simple ordered compounds, identifying ionic transport pathways in disordered compounds requires considering two additional levels of complexity namely: (a) connectivity through lowest barrier channels between hopping sites and (b) the varied energy landscape of the hopping sites itself.

We would like to thank Zinab Jadidi for discussions on the subject of transport and Li-TM interactions in DRX compounds. This work was supported by the U.S. Department of Energy, Office of Science, Basic Energy Sciences, Materials Sciences and Engineering Division under Contract No. DE-AC02-05-CH11231 within the (GENESIS EFRC) program (DE-SC0019212). T.C. acknowledges financial support from the Assistant Secretary for Energy Efficiency and Renewable Energy, Vehicle Technologies Office, under the Applied Battery Materials Program, of the U.S. Department of Energy (DOE) under Contract No. DE-AC02-05CH11231. The computational analysis was performed using computational resources of the National Energy Research Scientific Computing Center (NERSC), a DOE Office of Science User Facility supported by the Office of Science of the US Department of Energy under contract no. DE-C02-05CH11231.

-
- [1] M. D. Radin, S. Hy, M. Sina, C. Fang, H. Liu, J. Vinckeviciute, M. Zhang, M. S. Whittingham, Y. S. Meng, and A. Van der Ven, Narrowing the gap between theoretical and practical capacities in li-ion layered oxide cathode materials, *Advanced Energy Materials* **7**, 1602888 (2017).
- [2] J. H. Yang, H. Kim, and G. Ceder, Insights into layered oxide cathodes for rechargeable batteries, *Molecules* **26**, 3173 (2021).
- [3] E. A. Olivetti, G. Ceder, G. G. Gaustad, and X. Fu, Lithium-ion battery supply chain considerations: analysis of potential bottlenecks in critical metals, *Joule* **1**, 229 (2017).
- [4] A. Tolcin, Mineral commodity summaries 2019, US Geological Survey: Virginia, VA, USA , 74 (2011).
- [5] J. Lee, A. Urban, X. Li, D. Su, G. Hautier, and G. Ceder, Unlocking the potential of cation-disordered oxides for rechargeable lithium batteries, *science* **343**, 519 (2014).
- [6] N. Yabuuchi, M. Takeuchi, M. Nakayama, H. Shiiba, M. Ogawa, K. Nakayama, T. Ohta, D. Endo, T. Ozaki, T. Inamasu, *et al.*, High-capacity electrode materials for rechargeable lithium batteries: Li₃NbO₄-based system with cation-disordered rocksalt structure, *Proceedings of the National Academy of Sciences* **112**, 7650 (2015).
- [7] R. Chen, S. Ren, M. Knapp, D. Wang, R. Witter, M. Fichtner, and H. Hahn, Disordered lithium-rich oxyfluoride as a stable host for enhanced li+ intercalation storage, *Advanced Energy Materials* **5**, 1401814 (2015).
- [8] A. Urban, I. Matts, A. Abdellahi, and G. Ceder, Computational design and preparation of cation-disordered oxides for high-energy-density li-ion batteries, *Advanced Energy Materials* **6**, 1600488 (2016).
- [9] W. H. Kan, D. Chen, J. K. Papp, A. K. Shukla, A. Huq, C. M. Brown, B. D. McCloskey, and G. Chen, Unravelling solid-state redox chemistry in li_{1.3}nb_{0.3}mn_{0.4}o₂ single-crystal cathode material, *Chemistry of Materials* **30**, 1655 (2018).
- [10] J. Lee, D. A. Kitchaev, D.-H. Kwon, C.-W. Lee, J. K. Papp, Y.-S. Liu, Z. Lun, R. J. Clement, T. Shi, B. D. McCloskey, *et al.*, Reversible mn²⁺/mn⁴⁺ double redox in lithium-excess cathode materials, *Nature* **556**, 185 (2018).
- [11] J. Lee, D.-H. Seo, M. Balasubramanian, N. Twu, X. Li, and G. Ceder, A new class of high capacity cation-disordered oxides for rechargeable lithium batteries: Li-ni-ti-mo oxides, *Energy & Environmental Science* **8**, 3255 (2015).
- [12] L. Li, Z. Lun, D. Chen, Y. Yue, W. Tong, G. Chen, G. Ceder, and C. Wang, Fluorination-enhanced surface stability of cation-disordered rocksalt cathodes for li-ion batteries, *Advanced Functional Materials* **31**, 2101888 (2021).
- [13] J. Lee, J. K. Papp, R. J. Clément, S. Sallis, D.-H. Kwon, T. Shi, W. Yang, B. D. McCloskey, and G. Ceder, Mitigating oxygen loss to improve the cycling performance

- of high capacity cation-disordered cathode materials, *Nature communications* **8**, 1 (2017).
- [14] R. Clément, Z. Lun, and G. Ceder, Cation-disordered rocksalt transition metal oxides and oxyfluorides for high energy lithium-ion cathodes, *Energy & Environmental Science* **13**, 345 (2020).
- [15] Z. Lun, B. Ouyang, D.-H. Kwon, Y. Ha, E. E. Foley, T.-Y. Huang, Z. Cai, H. Kim, M. Balasubramanian, Y. Sun, *et al.*, Cation-disordered rocksalt-type high-entropy cathodes for li-ion batteries, *Nature materials* **20**, 214 (2021).
- [16] J. Huang, P. Zhong, Y. Ha, D.-H. Kwon, M. J. Crafton, Y. Tian, M. Balasubramanian, B. D. McCloskey, W. Yang, and G. Ceder, Non-topotactic reactions enable high rate capability in li-rich cathode materials, *Nature Energy* **6**, 706 (2021).
- [17] J. Ahn, Y. Ha, R. Satish, R. Giovine, L. Li, J. Liu, C. Wang, R. J. Clement, R. Kostecki, W. Yang, *et al.*, Exceptional cycling performance enabled by local structural rearrangements in disordered rocksalt cathodes, *Advanced Energy Materials* , 2200426 (2022).
- [18] H. Liu, Z. Zhu, Q. Yan, S. Yu, X. He, Y. Chen, R. Zhang, L. Ma, T. Liu, M. Li, *et al.*, A disordered rock salt anode for fast-charging lithium-ion batteries, *Nature* **585**, 63 (2020).
- [19] J. H. Chang, P. B. Jørgensen, S. Loftager, A. Bhowmik, J. M. G. Lastra, and T. Vegge, On-the-fly assessment of diffusion barriers of disordered transition metal oxyfluorides using local descriptors, *Electrochimica Acta* **388**, 138551 (2021).
- [20] A. Urban, J. Lee, and G. Ceder, The configurational space of rocksalt-type oxides for high-capacity lithium battery electrodes, *Advanced Energy Materials* **4**, 1400478 (2014).
- [21] H. Ji, A. Urban, D. A. Kitchaev, D.-H. Kwon, N. Artrith, C. Ophus, W. Huang, Z. Cai, T. Shi, J. C. Kim, *et al.*, Hidden structural and chemical order controls lithium transport in cation-disordered oxides for rechargeable batteries, *Nature communications* **10**, 1 (2019).
- [22] J. Lee, C. Wang, R. Malik, Y. Dong, Y. Huang, D.-H. Seo, and J. Li, Determining the criticality of li-excess for disordered-rocksalt li-ion battery cathodes, *Advanced Energy Materials* **11**, 2100204 (2021).
- [23] R. Chen, S. Ren, M. Yavuz, A. A. Guda, V. Shapovalov, R. Witter, M. Fichtner, and H. Hahn, Li⁺ intercalation in isostructural li₂vo₃ and li₂vo₂f with o²⁻ and mixed o^{2-/f-} anions, *Physical Chemistry Chemical Physics* **17**, 17288 (2015).
- [24] A. Van der Ven and G. Ceder, Lithium diffusion in layered lixcoo₂, *Electrochemical and Solid State Letters* **3**, 301 (2000).
- [25] M. Asta, C. Wolverton, D. De Fontaine, and H. Dreyssé, Effective cluster interactions from cluster-variation formalism. i, *Physical review B* **44**, 4907 (1991).
- [26] M. Andersen, C. Panosetti, and K. Reuter, A practical guide to surface kinetic monte carlo simulations, *Frontiers in chemistry* **7**, 202 (2019).
- [27] A. Van der Ven, G. Ceder, M. Asta, and P. Tepeesch, First-principles theory of ionic diffusion with nondilute carriers, *Physical Review B* **64**, 184307 (2001).
- [28] D. T. Gillespie, A general method for numerically simulating the stochastic time evolution of coupled chemical reactions, *Journal of computational physics* **22**, 403 (1976).
- [29] D. T. Gillespie, Exact stochastic simulation of coupled chemical reactions, *The journal of physical chemistry* **81**, 2340 (1977).
- [30] A. Van der Ven, Z. Deng, S. Banerjee, and S. P. Ong, Rechargeable alkali-ion battery materials: theory and computation, *Chemical Reviews* **120**, 6977 (2020).
- [31] S. K. Kolli and A. Van der Ven, Elucidating the factors that cause cation diffusion shutdown in spinel-based electrodes, *Chemistry of Materials* **33**, 6421 (2021).
- [32] A. Van der Ven, M. Aydinol, G. Ceder, G. Kresse, and J. Hafner, First-principles investigation of phase stability in lixcoo₂, *Physical Review B* **58**, 2975 (1998).
- [33] M. A. y de Dompablo, A. Van der Ven, and G. Ceder, First-principles calculations of lithium ordering and phase stability on lixnio₂, *Physical Review B* **66**, 064112 (2002).
- [34] A. Abdellahi, A. Urban, S. Dacek, and G. Ceder, Understanding the effect of cation disorder on the voltage profile of lithium transition-metal oxides, *Chemistry of Materials* **28**, 5373 (2016).
- [35] T. Chen, G. Sai Gautam, W. Huang, and G. Ceder, First-principles study of the voltage profile and mobility of mg intercalation in a chromium oxide spinel, *Chemistry of Materials* **30**, 153 (2018).
- [36] Z. Cai, H. Ji, Y. Ha, J. Liu, D.-H. Kwon, Y. Zhang, A. Urban, E. E. Foley, R. Giovine, H. Kim, *et al.*, Realizing continuous cation order-to-disorder tuning in a class of high-energy spinel-type li-ion cathodes, *Matter* **4**, 3897 (2021).
- [37] K. Luo, M. R. Roberts, R. Hao, N. Guerrini, D. M. Pickup, Y.-S. Liu, K. Edström, J. Guo, A. V. Chadwick, L. C. Duda, *et al.*, Charge-compensation in 3d-transition-metal-oxide intercalation cathodes through the generation of localized electron holes on oxygen, *Nature chemistry* **8**, 684 (2016).
- [38] J. Hong, W. E. Gent, P. Xiao, K. Lim, D.-H. Seo, J. Wu, P. M. Csernica, C. J. Takacs, D. Nordlund, C.-J. Sun, *et al.*, Metal-oxygen decoordination stabilizes anion redox in li-rich oxides, *Nature materials* **18**, 256 (2019).
- [39] N. Yabuuchi, M. Nakayama, M. Takeuchi, S. Komaba, Y. Hashimoto, T. Mukai, H. Shiiba, K. Sato, Y. Kobayashi, A. Nakao, *et al.*, Origin of stabilization and destabilization in solid-state redox reaction of oxide ions for lithium-ion batteries, *Nature communications* **7**, 1 (2016).
- [40] M. Freire, N. V. Kosova, C. Jordy, D. Chateigner, O. Lebedev, A. Maignan, and V. Pralong, A new active li-mn-o compound for high energy density li-ion batteries, *Nature materials* **15**, 173 (2016).
- [41] M. Freire, O. Lebedev, A. Maignan, C. Jordy, and V. Pralong, Nanostructured li₂mno₃: a disordered rock salt type structure for high energy density li ion batteries, *Journal of Materials Chemistry A* **5**, 21898 (2017).
- [42] J. Ahn, D. Chen, and G. Chen, A fluorination method for improving cation-disordered rocksalt cathode performance, *Advanced Energy Materials* **10**, 2001671 (2020).
- [43] Z. Jadidi, T. Chen, P. Xiao, A. Urban, and G. Ceder, Effect of fluorination and li-excess on the li migration barrier in mn-based cathode materials, *Journal of Materials Chemistry A* **8**, 19965 (2020).
- [44] H. Ji, J. Wu, Z. Cai, J. Liu, D.-H. Kwon, H. Kim, A. Urban, J. K. Papp, E. Foley, Y. Tian, *et al.*, Ultrahigh power and energy density in partially ordered lithium-ion cathode materials, *Nature Energy* **5**, 213 (2020).